Measurement of the Frequency of the $2^3S - 2^3P$ Transition of ^{4}He

X. Zheng[1,2], Y. R. Sun[1,2,*], J.-J. Chen[1], W. Jiang[2], K. Pachucki[3], and S.-M. Hu[1,2,*]
[1] *Hefei National Laboratory for Physical Sciences and Microscale, iChem Center, University of Science and Technology of China, Hefei, 230026, China*
[2] *CAS Center for Excellence and Synergetic Innovation Center in Quantum Information and Quantum Physics, University of Science and Technology of China, Hefei, 230026, China*
[3] *Faculty of Physics, University of Warsaw, Pasteura 5, 02-093, Warsaw, Poland*
(Dated: November 13, 2017)

The $2^3S - 2^3P$ transition of ^{4}He was measured by comb-linked laser spectroscopy using a transverse-cooled atomic beam. The centroid frequency was determined to be 276 736 495 600.0(1.4) kHz, with a fractional uncertainty of 5.1×10^{-12}. This value is not only more accurate but also differs by as much as -49.5 kHz (20 σ) from the previous result given by Cancio Pastor *et al.*, Phys. Rev. Lett. **92**, 023001 (2004); **97**, 139903(E) (2006); **108**, 143001 (2012). In combination with ongoing theoretical calculations, this work may allow the most accurate determination of the nuclear charge radius of helium.

Precision spectroscopy in few-body atomic systems, like hydrogen and helium, enables testing of the quantum electrodynamics (QED) theory and determination of the fundamental physical constants, such as the Rydberg constant [1–4], the proton charge radius [5], and the fine structure constant [6]. It also sets constraints on new physics beyond the Standard Model (BSM) [7, 8]. It is tempting to assume that BSM physics is responsible for the so-called proton radius puzzle, the discrepancy between muonic and electronic hydrogen spectroscopy [9]. However, no generally accepted model has been proposed so far [10]. Moreover, a very recent hydrogen result [11] is in agreement with the muonic value of the proton charge radius, not leaving much room for the BSM physics. Nevertheless, this striking discrepancy stimulates analogous measurements of muonic [12] and electronic hydrogen-like helium ions [13, 14]. The nuclear charge radius of He can be determined from muonic helium spectroscopy, provided that the nuclear polarizability can be accurately calculated. Moreover, a very narrow 1S-2S transition in electronic He^+ is almost free of the nuclear polarizability effects, but accurate measurements in the vacuum ultraviolet region (30 nm) are very challenging.

High-precision spectroscopy of atomic helium, as presented in this Letter, combined with ongoing theoretical calculations for the point nucleus may allow an alternative determination of the helium nuclear charge radius, which could be more accurate than from the electron scattering [15, 16]. Moreover, the comparison of results from electronic and muonic helium will provide a sensitive test of universality in the electromagnetic interactions of leptons [17].

The $2^3S - 2^3P$ transition of He is particularly suitable for this purpose because it is relatively sensitive to the nuclear charge radius and can be calculated within the QED theory up to the $\alpha^7 m$ order. These calculations will bring the theoretical accuracy to the 10-kHz level and may allow determination of the helium nuclear charge radius with an accuracy of 10^{-3} [18]. The centroid frequency of the $2^3S - 2^3P$ transition has been measured with a stated uncertainty of 2.1 kHz by Cancio Pastor *et al.* using saturated-fluorescence spectroscopy [19, 20]. The same method was applied to determine the $2^3S - 2^3P$ centroid of ^{3}He and the difference of the squared nuclear charge radii δr^2 between ^{3}He and ^{4}He [20]. However, the obtained δr^2 differs from that obtained from the $2^3S - 2^1S$ transition [21] by 4σ, and this discrepancy remains unexplained [22, 23].

In this Letter, we report on the laser spectroscopy measurement of the $2^3S - 2^3P$ transition of ^{4}He in an atomic

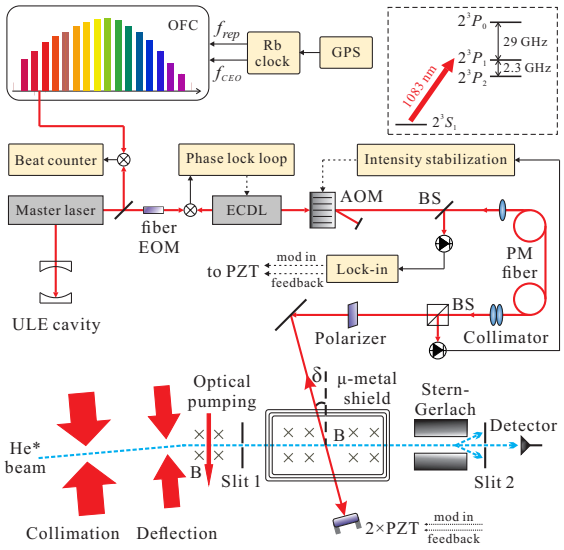

FIG. 1. Schematic of the beam apparatus and the optical layout. Inset: the energy levels of the $2^3S - 2^3P$ transitions. AOM: acoustic-optical modulator; BS: beam splitter; ECDL: external cavity diode laser; EOM: electro-optical modulator; GPS: global positioning system; OFC: optical frequency comb; PM: polarization maintaining; PZT: piezoelectric transducer; ULE: Ultra-low expansion.

* Corresponding authors: robert@mail.ustc.edu.cn (Y.R.S.); smhu@ustc.edu.cn (S.-M.H.)

beam. The configuration of the experimental setup is shown in Fig. 1. It is similar to the one presented in our previous studies [24, 25] and thus, will be briefly described here. Helium atoms in the 2^3S_1 metastable state were produced by radio-frequency (RF) discharge and subsequently collimated by two-dimensional transverse cooling by a laser in resonance with the $2^3S_1 - 2^3P_2$ transition. A second transverse-cooling field deflected the atoms in the triplet state (2^3S_1) from the original beam by an angle of 0.1°. Two slits with a width of 0.5 mm were placed 1.5 m apart in the beam. The first slit was positioned after the beam-deflecting region, and the second slit was placed before the detector. As a result, the background particles, including the helium atoms in the 2^1S_0 singlet state and the UV photons, were removed from the beam [26–28]. A linearly polarized laser beam was tuned to be in resonance with the $2^3S_1 - 2^3P_0$ transition and was used for optical pumping. When the atoms reached the spectroscopy region, over 99% of the helium atoms at the $2^3S_1(m = 0)$ level were transferred to either the $m = -1$ or the $m = +1$ level. The $2^3S_1(m = 0)$ state was repopulated when the atoms interacted with the probe laser which scanned through the resonance of the $2^3S_1 - 2^3P_J$ $(J = 0, 1, 2)$ transition. This spectroscopy region was shielded with three layers of cylindrically shaped μ metal. A homogeneous magnetic field was generated inside the magnetic shield by a cosine theta coil [29], which arranged the current density in a cosine theta distribution. Between the spectroscopy region and the detector, a Stern−Gerlach magnet was used to deflect atoms at the $m = \pm 1$ levels to ensure that only the atoms at the $m = 0$ level could pass through the second slit and reach the detector.

A narrow-band fiber laser was used as the master laser, and was locked with an etalon composed of ultra-low-expansion glass. The absolute frequency of the master laser was determined according to the beat with an optical frequency comb. The comb was synthesized by a Er:fiber oscillator operating at 1.56 μm and its repetition frequency and carrier offset frequency were both referenced to a GPS-disciplined rubidium clock (SRS FS725). The probe laser − an external-cavity diode laser (ECDL) − was phase-locked with the master laser. To extend the tuning range to cover all the $2^3S_1 - 2^3P_J$ $(J = 0, 1, 2)$ transitions, a fiber EOM was used to produce sidebands up to 16 GHz driven by an RF synthesizer (R&S SMB100A). The probe laser beam was coupled into a polarization-maintaining fiber and a noise-eater for power stabilization. The probe laser power fluctuation was below 0.1% and was kept less than one quarter of the saturation intensity (167 μW cm^{-2}). In the spectroscopy region, the probe beam was aligned perpendicular to the atomic beam and retro-reflected to compensate for the first-order Doppler shift.

The spectra were recorded by scanning the probe laser frequency in a random order. A bias magnetic field of 5 - 20 Gauss was applied during the scan. A sample spectrum of the $2^3S_1 - 2^3P_1$ transition is shown in Fig. 2. Two peaks rising from the $m = +1$ and $m = -1$ sublevels, respectively, were obtained and their centers were derived from fitting the peaks with a Lorentzian profile. The transition frequency was determined from the average of the two peak centers, which cancelled the first-order Zeeman shifts. The measurements were taken at different probe laser intensities, and the final value of $f_1\,(2^3S_1 - 2^3P_1)$ was derived by extrapolating to the zero laser power. In total, about 9000 spectra of the $2^3S_1 - 2^3P_1$ transition were recorded during 23 consecutive days in April and 11 days in July of 2017. The results are depicted in Fig. 3.

The first-order Doppler (FOD) shift because of the misalignment of the probe laser, which is exaggerated in Fig. 1 by an angle δ, must be considered in the measurement. Counter-propagating probe laser beams were used in the measurements to reduce the FOD shift. Before

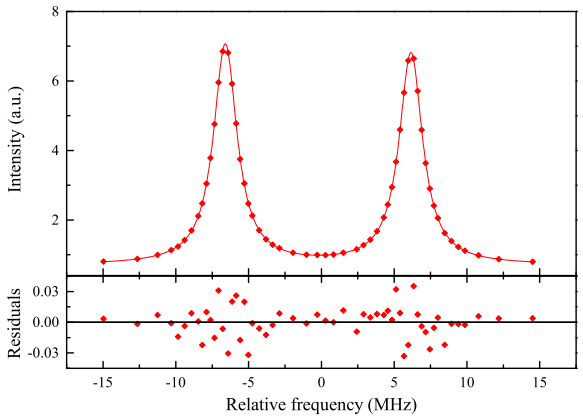

FIG. 2. Spectrum from a single scan with a probe laser power of 1.20 μW. The solid line is the simulated spectrum from fitting the data with Lorentzian functions. Residuals of the fit are shown in the lower panel.

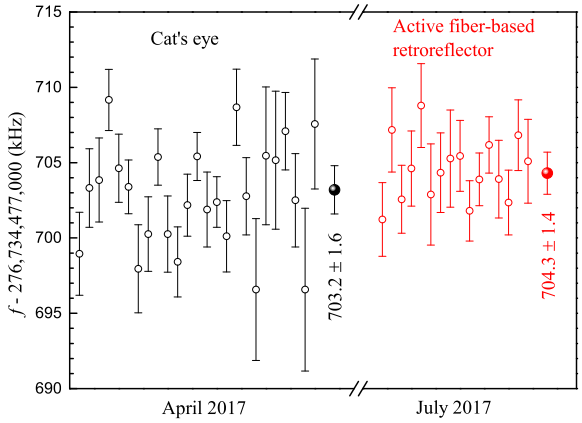

FIG. 3. Comparison of the 41 independent measurements of $2^3S_1 - 2^3P_1$ transition frequency in April and July using the two different approaches. Each open point represents an average per measurement. The labeled filled points are the weighted mean values including systematic uncertainties.

each measurement, spectra with and without the retro-reflected probe beam were recorded and the line centers obtained from both spectra were compared to ensure that the difference was below 20 kHz, corresponding to a δ of less than 30 μrad. However, any imperfection of the retro-reflection led to a residual Doppler shift:

$$\Delta f_{\rm res} = \frac{1}{2}\frac{v}{\lambda}[\sin(\delta+\varepsilon) - \sin(\delta)] \approx \frac{v}{2\lambda}\varepsilon. \qquad (1)$$

where v was the velocity of the atoms and ε was the angle between the misaligned "counter-propagating" laser beams.

To reduce the FOD shift, retro-reflected probe beam had to be optimized to reduce ε. Two different approaches were used. One was the "cat's eye" method [30], which was used in 25 individual measurements taken in April 2017 (see Fig. 3). The other one was the "active fiber-based retroreflector" method (AFR) introduced by Beyer *et al.* [31]. A feedback servo was used to control a PZT-modulated mirror to reflect the probe laser beam, which is shown in Fig. 1. The "AFR" method was used in 16 measurements taken in July 2017. Before each measurement, the retro-reflecting setup was dismantled and reinstalled. The possible shift from the wavefront distortions was also checked by using collimators with different focal lengths. The results obtained from these two methods are shown in Fig. 3. The uncertainty of the results obtained with the "AFR" method is lower than that from the "cat's eye" method. The deviation between the averaged values from both methods is within the joint uncertainty.

To assess the residual FOD shift, the longitudinal velocity distribution of the helium atoms in the beam was also analyzed. The $2^3S - 2^3P$ transition was excited at an incident angle δ (see Fig. 1) of about 3°, and the first-order Doppler shift was used to determine the velocity of the atomic beam (see *Supplemental Material* [32]). This transition had a sufficiently narrow natural linewidth (1.6 MHz) to resolve the velocities. The accuracy of the δ angle was about 0.2°, which translated to an uncertainty of about 10% in the absolute velocity. The atomic beam with optimized intensity had a mean velocity of about 700 m/s, which was used in most measurements. Test measurements with different distributions were also run by changing the deflection angle of the atomic beam and the positions of the two slits. The distributions with mean velocities of 700 m/s, 570 ms/s, and 830 m/s are shown in Fig. 4(a). About 1000, 3500, and 3500 spectra were recorded at these conditions, respectively, and the $f_1\,(2^3S_1 - 2^3P_1)$ values determined from the corresponding spectra are shown in Fig. 4(b). They agree well with each other. Since the deviation was only 0.36 kHz under a change of about one third of the mean velocity, the residual first-order Doppler shift was estimated to be 1.1 kHz, corresponding to a misalignment angle ε of 3 μrad.

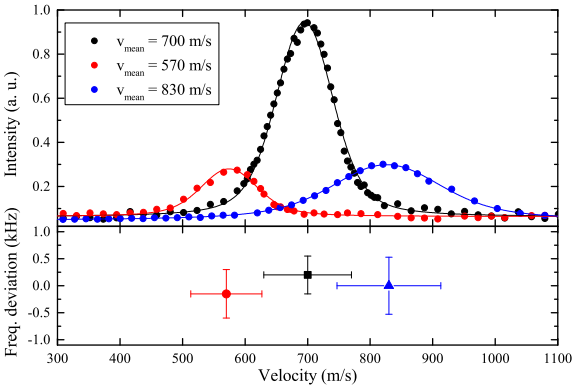

FIG. 4. (a) Longitudinal velocity distribution profiles of the 2^3S_1 atoms recorded at different deflection angles with Voigt fit. (b) Frequency deviations of the $2^3S_1 - 2^3P_1$ transition recorded under different conditions. Each point is weighted averaged with corrections, and the error bar represents the 1σ statistical uncertainty.

Other contributions to the uncertainty budget are summarized in Table I.

(1) The second-order Doppler shift was calculated as $v^2 f_1/(2c^2)$. The mean velocity was measured with an uncertainty of 70 m/s or less, leading to an uncertainty of 0.15 kHz.

(2) The frequency calibration was limited by the GPS-disciplined rubidium clock, which had a relative uncertainty of 2×10^{-12}, or 550 Hz at 276 THz. The frequency drift of the master laser was determined from its beat with the comb, which was below 3 kHz/hr. Because each spectral scan took about 80 s, the error due to the frequency drift was negligible.

(3) The retro-reflected probe laser beam had a power loss of about 5% because of the imperfect anti-reflection coated viewports, which led to asymmetry in the recorded spectral line profile. It should be noted that the incident angle of the probe laser beam (δ) was below 30 μrad, and simulation showed that the uncertainty because of the line profile asymmetry was less than 0.3 kHz.

(4) The quantum interference effect [33–38] arises from

TABLE I. Uncertainty budget of the $2^3S_1 - 2^3P_1$ transition frequency (f_1), in kHz.

Source	Corrections	$\Delta f(1\sigma)$
Statistics		0.45
First-order Doppler		1.1
Second-order Doppler	+0.70	0.15
Frequency calibration		0.55
Line profile		0.30
Quantum interference	+0.60	0.10
Laser power		0.10
Zeeman effect[a]		0.01
Recoil shift	−42.20	–
Total	276 734 477 703.8	1.4

[a] The second-order Zeeman corrections have already been included.

TABLE II. Experimental results of the $2^3S_1 - 2^3P_{0,1,2}$ transitions, in kHz.

	f_0	f_1	f_2	f_c
This work	276 764 094 657.2(1.4)	276 734 477 703.8(1.4)	276 732 186 526.2(1.4)	276 736 495 600.0(1.4)
Cancio Pastor *et al.* [19]	276 764 094 707.3(2.1)	276 734 477 752.5(2.0)	276 732 186 620.5(15.0)	276 736 495 649.5(2.1)[a]

[a] Centroid frequency was reevaluated in Ref. [20].

near-resonant energy levels. We took a similar approach as with our previous studies, and the corrections for the $2^3S_1 - 2^3P_J$ transitions were obtained as +0.08(3), +0.60(10), and −0.60(10) kHz for $J = 0$, 1, and 2, respectively. A detailed calculation is presented in the *Supplemental Material* [32].

(5) The pressure of the background gases in the spectroscopy region was about 10^{-5} Pa. Because the pressure shift had been calculated to be −14 kHz/Pa [39], it could be safely neglected under the experimental conditions present at the time.

(6) The recoil shift correction was $\Delta f_{recoil} = -h/(2m\lambda^2) = -42.2$ kHz and the uncertainty was negligible.

(7) Other contributions to the uncertainty budget, including the laser power, Zeeman effect, and the scattering light, have been discussed in our previous studies [24, 25], and they were similar in this work. The first-order Zeeman shift cancelled out, and the second-order Zeeman correction could be calculated precisely [40]. The contribution from the residual magnetic field (<0.3 mG) was less than 10 Hz. No evidence was found for the AC Stark shift resulting from the scattering light from the pumping laser.

As given in Table II, the $2^3S_1 - 2^3P_1$ transition frequency (f_1) was determined to be 276 734 477 703.8(1.4) kHz. The frequencies of the transitions $2^3S_1 - 2^3P_0$ (f_0) and $2^3S_1 - 2^3P_2$ (f_2) were derived by combining f_1 with the 2^3P_J fine-structure intervals given in our previous study [25]. Using the same method as in f_1, we also measured the frequencies of f_0 and f_2, which agree well with those given in Table II, with deviations of +0.7(2.1) kHz and +1.1(2.1) kHz, respectively [32]. The centroid frequency of the $2^3S - 2^3P$ transition was derived as:

$$f_c = \frac{\sum_J (2J+1) f_J}{\sum_J (2J+1)} \qquad (2)$$
$$= 276\,736\,495\,600.0 \pm 0.45(\text{stat}) \pm 1.3(\text{syst}) \text{ kHz},$$

The $2^3S_1 - 2^3P_J$ frequencies reported by Cancio Pastor *et al.* [19] are also given in Table II. Their f_c value was reevaluated in Ref. [20] with a stated uncertainty of 2.1 kHz, which differs from this work by 49.5 kHz (20σ). The fine-structure intervals ν_{02} and ν_{12} obtained by Cancio Pastor *et al.* differ from the results obtained in our previous study [25] by about 45 kHz [32]. Such a large discrepancy, existing in the fine-structure intervals involving 2^3P_2, could be due to their less accurate f_2 value which has a stated uncertainty of 15 kHz. The

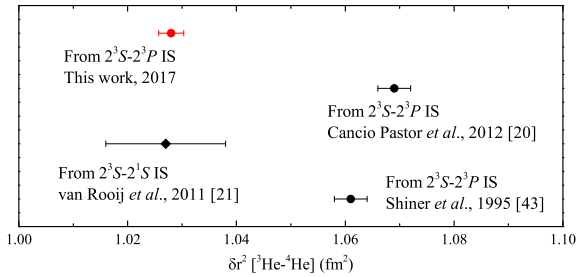

FIG. 5. Comparison of the difference of squared nuclear charge radii between ^{3}He and ^{4}He (see details in the text). IS, isotope shift.

ν_{01} interval given by Cancio Pastor *et al.* agrees with our previous result, indicating a possible common systematic shift of f_0 and f_1 between both studies.

The theoretical 2^3S-2^3P transition centroid frequency given by Pachucki *et al.* [17] is 276 736 495.4(2.0) MHz, which is only 0.2 MHz lower than the value obtained in this work. The 2-MHz uncertainty mainly arose from the yet-unknown $\alpha^7 m$ QED corrections. It should be noted that the ionization energy of the 3^3D_1 state has been calculated as 366 018 892.97(2) MHz by Drake's group [41], with a stated uncertainty of 20 kHz. Using that value, the ionization energies of the 2^3S and 2^3P states can be derived using the $2^3P_0 - 3^3D_1$ frequency measured by Luo *et al.* [42] and the $2^3S - 2^3P$ frequencies determined in this work. Values of 1 152 842 742.979(34) MHz and 876 106 247.379(34) MHz were obtained, respectively, which are larger than the recent theoretical results [17] by 1.6(1.3) MHz and 1.4(0.7) MHz, correspondingly. This implies that reinvestigation of the 3^3D state is needed.

The $2^3S - 2^3P$ centroid frequency of ^{4}He reported by Cancio Pastor *et al.* and the value of ^{3}He centroid given in Ref. [20] have been used to derive the isotope shift which yields the difference of the squared nuclear charge radii δr^2 value of 1.069(3) fm^2. Interestingly, if we replace their $2^3S - 2^3P$ centroid frequency of ^{4}He with the value obtained in this work, the resulting δr^2 value will be 1.028(2) fm^2, which agrees well with the value of 1.027(11) fm^2 derived from the isotope shift in the $2^3S - 2^1S$ transition measured by van Rooij *et al.* [21], but differs significantly with that of 1.061(3) fm^2 from an earlier study of the $2^3S - 2^3P$ isotope shift measured by Shiner *et al.* [43]. Note that the updated theoretical values [17] have been adopted in the calculation of the results given here. A comparison of these results is shown

in Fig. 5. More details of the calculation are given in the *Supplemental Material* [32]. The significant deviations between these results indicate the need for further independent measurements of He isotope shifts. We are also constructing a new beamline for the frequency metrology of the $2^3S - 2^3P$ transitions of ^{3}He.

The new $2^3S - 2^3P$ frequency obtained in this work, which completely disagrees with the result of the previous study reported in Refs. [19, 20], may lead to a determination of the nuclear charge radius of He ($r_{\rm He}$) with a relative accuracy of 10^{-3}, once the theoretical calculations for $\alpha^7 m$ corrections have been accomplished. This will enable a comparison of the $r_{\rm He}$ values obtained from electronic helium spectroscopy with those from electron scattering, and from muonic helium in the future. Such a comparison will help to resolve the proton charge radius puzzle, while in the case of disagreement with muonic determination it will open a window for new physics beyond the Standard Model by violation of the lepton universality in electromagnetic interactions.

ACKNOWLEDGMENTS

The authors from USTC are indebted to Dr. Haifeng Jiang from the National Time Service Center for his help on the optical frequency comb. This work is jointly supported by the Chinese Academy of Science (XDB21010400, XDB21020100), the Natural Science Foundation of China (91736101, 21688102, 11304303, 91436209, 21427804), and the Ministry of Science and Technology of China (2013CB834602). K.P. acknowledges support from the National Science Center of Poland (Grant No. 2012/04/A/ST2/00105).

[1] C. G. Parthey, A. Matveev, J. Alnis, B. Bernhardt, A. Beyer, R. Holzwarth, A. Maistrou, R. Pohl, K. Predehl, T. Udem, T. Wilken, N. Kolachevsky, M. Abgrall, D. Rovera, C. Salomon, P. Laurent, and T. W. Hänsch, Phys. Rev. Lett. **107**, 203001 (2011).
[2] A. Matveev, C. G. Parthey, K. Predehl, J. Alnis, A. Beyer, R. Holzwarth, T. Udem, T. Wilken, N. Kolachevsky, M. Abgrall, D. Rovera, C. Salomon, P. Laurent, G. Grosche, O. Terra, T. Legero, H. Schnatz, S. Weyers, B. Altschul, and T. W. Hänsch, Phys. Rev. Lett. **110**, 230801 (2013).
[3] B. de Beauvoir, F. Nez, L. Julien, B. Cagnac, F. Biraben, D. Touahri, L. Hilico, O. Acef, A. Clairon, and J. J. Zondy, Phys. Rev. Lett. **78**, 440 (1997).
[4] C. Schwob, L. Jozefowski, B. de Beauvoir, L. Hilico, F. Nez, L. Julien, F. Biraben, O. Acef, J.-J. Zondy, and A. Clairon, Phys. Rev. Lett. **82**, 4960 (1999).
[5] F. Biraben, Euro. Phys. J. Spec. Topics **172**, 109 (2009).
[6] K. Pachucki and V. A. Yerokhin, Phys. Rev. Lett. **104**, 070403 (2010).
[7] E. J. Salumbides, J. C. J. Koelemeij, J. Komasa, K. Pachucki, K. S. E. Eikema, and W. Ubachs, Phys. Rev. D **87**, 112008 (2013).
[8] F. Ficek, D. F. J. Kimball, M. G. Kozlov, N. Leefer, S. Pustelny, and D. Budker, Phys. Rev. A **95**, 032505 (2017).
[9] R. Pohl, A. Antognini, F. Nez, F. D. Amaro, F. Biraben, J. M. R. Cardoso, D. S. Covita, A. Dax, S. Dhawan, L. M. P. Fernandes, A. Giesen, T. Graf, T. W. Hänsch, P. Indelicato, L. Julien, C.-Y. Kao, P. Knowles, E.-O. Le Bigot, Y.-W. Liu, J. M. Lopes, L. Ludhova, C. M. B. Monteiro, F. Mulhauser, T. Nebel, P. Rabinowitz, J. M. F. dos Santos, L. A. Schaller, K. Schuhmann, C. Schwob, D. Taqqu, J. F. C. A. Veloso, and F. Kottmann, Nature **466**, 213 (2010).
[10] R. Pohl, R. Gilman, G. A. Miller, and K. Pachucki, Annu. Rev. Nuc. Part. Sci. **63**, 175 (2013).
[11] A. Beyer, L. Maisenbacher, A. Matveev, R. Pohl, K. Khabarova, A. Grinin, T. Lamour, D. C. Yost, T. W. Hänsch, N. Kolachevsky, and T. Udem, Science **358**, 79 (2017).
[12] A. Antognini, F. Biraben, J. M. Cardoso, D. S. Covita, A. Dax, L. M. Fernandes, A. L. Gouvea, T. Graf, T. W. Hänsch, M. Hildebrandt, P. Indelicato, L. Julien, K. Kirch, F. Kottmann, Y.-W.-W. Liu, C. M. Monteiro, F. Mulhauser, T. Nebel, F. Nez, J. M. S. dos Santos, K. Schuhmann, D. Taqqu, J. F. Veloso, A. Voss, and R. Pohl, Can. J. Phys. **89**, 47 (2011).
[13] M. Herrmann, M. Haas, U. D. Jentschura, F. Kottmann, D. Leibfried, G. Saathoff, C. Gohle, A. Ozawa, V. Batteiger, S. Knünz, N. Kolachevsky, H. A. Schüssler, T. W. Hänsch, and T. Udem, Phys. Rev. A **79**, 052505 (2009).
[14] R. K. Altmann, S. Galtier, L. S. Dreissen, and K. S. E. Eikema, Phys. Rev. Lett. **117**, 173201 (2016).
[15] C. Ottermann, G. Köbschall, K. Maurer, K. Röhrich, C. Schmitt, and V. Walther, Nucl. Phys. A **436**, 688 (1985).
[16] I. Sick, J. Phys. Chem. Ref. Data **44**, 031213 (2015).
[17] K. Pachucki, V. c. v. Patkóš, and V. A. Yerokhin, Phys. Rev. A **95**, 062510 (2017).
[18] V. c. v. Patkóš, V. A. Yerokhin, and K. Pachucki, Phys. Rev. A **94**, 052508 (2016).
[19] P. C. Pastor, G. Giusfredi, P. D. Natale, G. Hagel, C. de Mauro, and M. Inguscio, Phys. Rev. Lett. **92**, 023001 (2004); *ibid.* **97**, 139903 (2006).
[20] P. Cancio Pastor, L. Consolino, G. Giusfredi, P. De Natale, M. Inguscio, V. A. Yerokhin, and K. Pachucki, Phys. Rev. Lett. **108**, 143001 (2012).
[21] R. van Rooij, J. S. Borbely, J. Simonet, M. D. Hoogerland, K. S. E. Eikema, R. A. Rozendaal, and W. Vassen, Science **333**, 196 (2011).
[22] K. Pachucki and V. A. Yerokhin, J. Phys. Chem. Ref. Data **44**, 031206 (2015).
[23] W. Vassen, R. P. M. J. W. Notermans, R. J. Rengelink, and R. F. H. J. v. d. Beek, Appl. Phys. B **122**, 289 (2016).
[24] G.-P. Feng, X. Zheng, Y. R. Sun, and S.-M. Hu, Phys. Rev. A **91**, 030502 (2015).
[25] X. Zheng, Y. R. Sun, J.-J. Chen, W. Jiang, K. Pachucki, and S.-M. Hu, Phys. Rev. Lett. **118**, 063001 (2017).
[26] N. Vansteenkiste, C. Gerz, R. Kaiser, L. Hollberg, C. Salomon, and A. Aspect, J. Phys. II France **1**, 1407 (1991).
[27] W. Rooijakkers, W. Hogervorst, and W. Vassen, Opt.

Communications **123**, 321 (1996).
[28] Y. R. Sun, G.-P. Feng, C.-F. Cheng, L.-Y. Tu, H. Pan, G.-M. Yang, and S.-M. Hu, Acta Phys. Sin. **61**, 170601 (2012).
[29] L. Bolinger, M. G. Prammer, and J. S. Leigh, J. Mag. Res. **81**, 162 (1989).
[30] P. Mueller, L.-B. Wang, G. W. F. Drake, K. Bailey, Z.-T. Lu, and T. P. O'Connor, Phys. Rev. Lett. **94**, 133001 (2005).
[31] A. Beyer, L. Maisenbacher, A. Matveev, R. Pohl, K. Khabarova, Y. Chang, A. Grinin, T. Lamour, T. Shi, D. C. Yost, T. Udem, T. W. Hänsch, and N. Kolachevsky, Opt. Express **24**, 17470 (2016).
[32] See *Supplemental Material* for details.
[33] A. Marsman, M. Horbatsch, and E. A. Hessels, Phys. Rev. A **86**, 040501 (2012).
[34] A. Marsman, E. A. Hessels, and M. Horbatsch, Phys. Rev. A **89**, 043403 (2014).
[35] A. Marsman, M. Horbatsch, and E. A. Hessels, J. Phys. Chem. Ref. Data **44**, 031207 (2015).
[36] C. J. Sansonetti, C. E. Simien, J. D. Gillaspy, J. N. Tan, S. M. Brewer, R. C. Brown, S. Wu, and J. V. Porto, Phys. Rev. Lett. **107**, 023001 (2011).
[37] R. C. Brown, S. Wu, J. V. Porto, C. J. Sansonetti, C. E. Simien, S. M. Brewer, J. N. Tan, and J. D. Gillaspy, Phys. Rev. A **87**, 032504 (2013).
[38] M. Kleinert, M. E. Gold Dahl, and S. Bergeson, Phys. Rev. A **94**, 052511 (2016).
[39] D. Vrinceanu, S. Kotochigova, and H. R. Sadeghpour, Phys. Rev. A **69**, 022714 (2004).
[40] Z.-C. Yan and G. W. F. Drake, Phys. Rev. A **50**, R1980 (1994).
[41] D. C. Morton, Q. Wu, and G. W. Drake, Can. J. Phys. **84**, 83 (2006).
[42] P.-L. Luo, J.-L. Peng, J. Hu, Y. Feng, L.-B. Wang, and J.-T. Shy, Phys. Rev. A **94**, 062507 (2016).
[43] D. Shiner, R. Dixson, and V. Vedantham, Phys. Rev. Lett. **74**, 3553 (1995).